Theoretical and experimental analysis of high Q SAW resonator transient response in a wireless sensor interrogation application

P. Varshney,
B.S. Panwar, P. Rathore
CARE, Indian Institute of Technology Delhi
New Delhi, India
Email: varshney.pratyush@gmail.com

S. Ballandras,
B. François, G. Martin
FEMTO-ST, UMR CNRS 6174,
Univ. of Franche Comté,
Besançon, France
Email: ballandr@femto-st.fr

J.-M. Friedt, T.Rétornaz
SENSeOR SAS,
Besançon, France

***Abstract*— Wireless sensing using SAW resonators calls for an accurate modeling and simulation of the charging and discharging of a resonator, connected to a resonant antenna (monopole/dipole) as a source/load. It is well known that a resonator takes about Q/π time periods of the natural resonant frequency to charge/discharge appreciably. The charging and discharging is critically affected by the static capacitance and the antenna impedance. The present work describes the theoretical modeling and experimental validation of the charging and discharging steps of a high Q SAW resonator in a wireless protocol and loading/unloading transients under variable load conditions are estimated. Furthermore, interrogation range using a monostatic RADAR-like reader (+10 dBm emitted power in the 434 MHz ISM band, -60 dBm detection limit) is estimated in air, dielectric media with or without conducting term, consistent with experimental measurements at 3 m in air when using a monopole antenna, 12 m when using directive Yagi-Uda antenna on the interrogation unit (monopole on the sensor side), 40 cm in tap water, negligible distance in sea water.**

Keywords: SAW, resonator, BVD, transient, anti-resonant, RADAR range

I. Introduction

Wireless sensor networks are increasingly becoming popular for industrial, health care and environmental monitoring applications. In many situations (e.g. rotating machine parts [1], patient monitoring [2]), the use of wires is impractical. In extremely harsh environments (high temperature [3], [4], pressure, radiation), the use of conventional sensors is impossible. In many applications, the sensors are buried in the structures and long lifetime necessitates battery less operation. Hence the motivation for developing wireless, passive sensor networks based on highly robust and wirelessly interrogable SAW devices.

Surface acoustic wave (SAW) devices have been conventionally used for IF bandpass filters, high quality resonators, pulse compression radars and similar RF signal processing [5]. Nowadays, they are becoming increasingly popular for passive wireless sensing applications [6]. SAW devices can store energy from the RF interrogation signal and reply back after some delay. The ambient conditions modify the properties of the surface waves propagating on the piezoelectric material (velocity, attenuation and reflection coefficient of the mirrors) and the returned signal can be analyzed for getting the sensed parameter (temperature [7], pressure [8], strain [9], torque [10], [11], mass loading by chemical species [12]). Conventionally, SAW/BAW resonators and delay lines are used for wireless sensing applications. The shift in the resonant frequency of the resonator and the phase shift of the delay line gives an estimate of the sensed parameter. High Q ($>$10000) resonators and wide-band delay lines can measure the sensed parameters with high accuracy (0.1 K, for eg.).

SAW resonators consist of an Interdigitated transducer (IDT) placed in a Fabry-Perot like cavity formed by shorted electrode gratings on both side, as shown in Fig 1.

Fig. 1. Structure of a synchronous resonator

The surface acoustic waves are excited by the IDT transducer placed in the cavity. The waves are reflected by the mirrors on both sides to form a standing wave pattern. The pitch and number of electrodes in the mirrors is selected to give strong reflections at a frequency (resonant frequency) around a narrow bandwidth (high Q factor). The gap in the cavity is adjusted to make the round trip phase shift an integer number of 360° (at the resonant frequency). This allows the resonator to store a large amount of energy around the resonant frequency.

SAW technology allow us to obtain high Q resonators at frequencies higher than possible with Quartz crystal resonators. This is because at high frequencies the substrate becomes exceedingly thin and fragile, while harmonic operation is not

efficient. The present work describes the theoretical modeling of SAW resonators using an electrical equivalent circuit [13], [14]. This helps to understand the relationship between the electrical and mechanical phenomenon in the SAW resonator. This circuit is used to model the exponential charging and discharging of a SAW resonator connected as a load/source to a dipole antenna.The transient response is used to model the performance of SAW resonator as a wireless sensor.

The steady state current in the motional branch of the resonator is taken as a measure of the mechanical energy stored in the resonator. A theoretical expression is derived for the time-constant and the energy storage by solving the relevant second order ODE subject to initial conditions. These values are used to estimate the link budget and hence the range of possible interrogation.Experimental assessment of the stated results is given, based on measurements of the power received by an interrogation unit used for the wireless interrogation of the SAW resonator. The continuity of current in the motional branch is theoretically and experimentally verified. The effect of static capacitance on the charging/discharging is modeled theoretically and experimentally. A theoretical expression is derived for the anti resonant frequency in terms of the BVD equivalent circuit parameters and compared with the actual observed values. This approach is finally used to scale the interrogation system performance for a given resonator, considering actual devices used for differential temperature measurements.

II. Butterworth-Van Dyke equivalent circuit

The SAW resonator shows a minimum impedance around the resonant frequency and a maximum impedance around a nearby anti-resonant frequency, with a very narrow fractional bandwidth (high Q). This behavior can be modeled by the BVD equivalent circuit model as shown in Fig. 2.

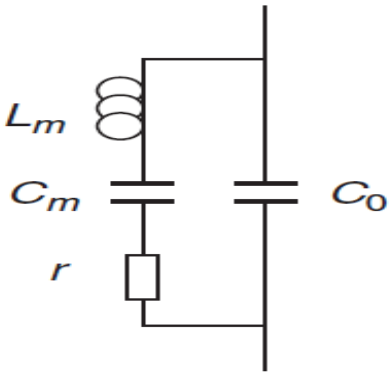

Fig. 2. BVD equivalent circuit

The BVD model consists of a series resonator LCR circuit in parallel with a capacitance C_0, which signifies the transducer capacitance. The inductance L_m and capacitance C_m are motional components associated with surface wave resonance, representing the exchange of mechanical energy between elastic potential energy of deformation and kinetic energy of particle motion. The maximum admittance is achieved at the resonant frequency $1/2\pi\sqrt{L_m C_m}$. Due to the parallel capacitance C_0, there is an admittance maxima at a nearby anti-resonant frequency [15].

A. Derivation of BVD model parameters

The admittance function of the BVD equivalent circuit is given by:

$$Y(\omega) = j\omega C_0 + \frac{1}{r + j(\omega L_m - 1/\omega C_m)} \tag{1}$$

We define, $\delta(\omega) = (\omega L_m - 1/\omega C_m)$

We can write,

$$Y(\omega) = \frac{r}{r^2 + \delta^2} + j(\omega C_0 - \frac{\delta}{r^2 + \delta^2})$$

At resonance, the imaginary part of admittance is zero. This leads to,

$$\omega C_0 = \frac{\delta}{r^2 + \delta^2}$$

Under suitable assumptions, we get,

$$f_r = \frac{1}{2\pi\sqrt{L_m C_m}},\ f_a = f_r(1 + \frac{C_m}{2C_0}) \tag{2}$$

where, f_r is resonant & f_a is anti-resonant frequency.
The 3 dB bandwidth of a series RLC circuit is given by,

$$B.W. = \frac{1}{2\pi}\frac{R}{L_m} \tag{3}$$

and the admittance of the resonator away from resonance:

$$Y(\omega) \approx j\omega C_0 \tag{4}$$

The step-by-step procedure for estimating the BVD model parameters from the measured S_{11} parameter – as provided by a wireless monostatic RADAR-like reader [16] – is given below:

1) Obtain Y parameters using $Y_{11} = \frac{1}{50}(\frac{1-S_{11}}{1+S_{11}})$
2) The maximum value of magnitude of Y_{11} occurs at resonant frequency, f_r
3) The minimum value of magnitude of Y_{11} occurs at anti-resonant frequency, f_a
4) The maximum of real(Y_{11}) gives $1/R$.
5) The width at half height of real(Y_{11}) gives the 3 dB bandwidth, B.W.
6) Using equation(3) we get L_m and then, using equation(2) we get C_m
7) We get the value of Y_{11} away from resonance and use equation(4) to get C_0

Hence, the BVD model parameters are completely determined. For an actual SAW resonator at 433.7 MHz (Q $\approx$ 14000), the estimated model parameters are given as: $C_0 = 5.17$ pF, $C_m = 0.84$ fF, $L_m = 0.16$ mH, $R = 31.6\ \Omega$. The actual and fitted values of the admittance parameter are shown in Fig.3.

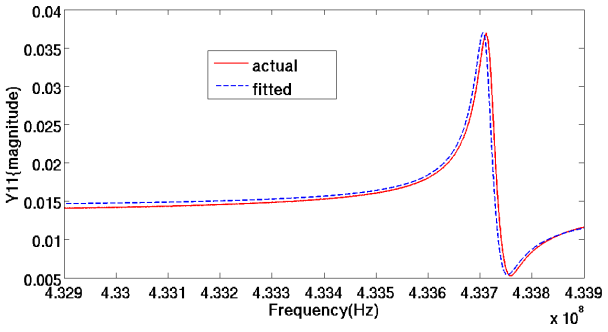

Fig. 3. Y_{11} parameter of actual resonator and from BVD model

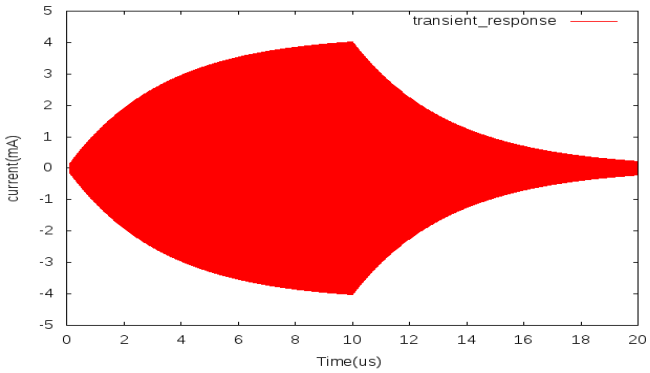

Fig. 4. Transient response of SAW resonator from ADS.

The fit is seen to determine the resonant frequency with an error of ≈ 6 kHz, associated with a temperature error of about 3 K when applied to a temperature sensor exhibiting a 2500 Hz/K sensitivity (SENSeOR SEAS10 sensor).

Although well suited to be implemented in low power embedded electronics, this analytical relationship fails in the case of a wireless link, in which the transmission line model must be added to the resonator. In this case, a least square error strategy must be used to identify all equivalent circuit parameters, yielding unknown computation time to reach convergence [17].

III. Transient Response of the Resonator

The second order differential equation describing the transient response of the SAW resonator can be written as:

$$L\frac{d^2q}{dt^2} + R\frac{dq}{dt} + \frac{1}{C}q = V_0\cos(\omega_0 t) \qquad (5)$$

The currents and voltages in the circuit reach their steady state values with a time constant of $2L/R$, which is equal to Q/π cycles of the resonant frequency. For the present case, it comes to ≈ 10 μs. This implies that it takes about 10 μs for the resonator to charge and discharge (exponentially) to 63% of its final value.

The transient response of the resonator is modelled in Agilent ADS. The ASCII text file containing the measured S_{11} parameters of the SAW resonator is read into the DATA ITEM component of ADS. The antenna is modelled as a 70 Ω load and the system is excited by a pulsed RF source of 10 μs duration, at the resonant frequency. After the source is switched off, the discharge of the resonator into the antenna is observed for another 10 μs. The step size for simulation is kept at 10 ps to capture the transient response faithfully [18]. Fig. 4 shows the simulated charging and discharging steps of the SAW resonator. Fig. 5 shows the experimentally measured transient response using a high sampling rate oscilloscope and a RF switch, to observe the charging and discharging transients.

The modelled transient response accurately matches the observed load and unload of an resonator subject to pulses defining a carrier frequency close to the resonance frequency, as done on a frequency-sweep wireless SAW sensor reader used to probe the returned power at each frequency within the 434 MHz European ISM band (Fig5).

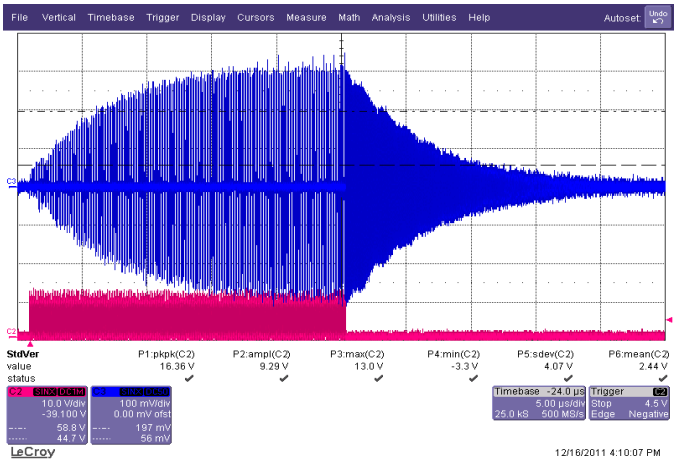

Fig. 5. Experimental load/unload of resonator: the carrier is chopped during load so that the stored energy is visible

IV. Interrogation Range Estimation

A. Propagation in air

For the wireless interrogation of SAW sensors, the maximum permissible level of transmitted power in the 433 MHz ISM band is 10 dBm. Generally, resonant monopoles and dipoles are used as antennas for the SAW resonator and directional antennas are used for the interrogation unit. The gain of sensor antennas can be taken as approx. unity for calculation of the range equation, while the interrogation unit antenna is modeled as having a gain G. The insertion loss of the SAW resonator (IL) is taken to be 3 dB. The round trip loss is calculated taking into account only the free space propagation loss (FSPL), the insertion loss of the resonator and the antenna gains, while neglecting the interrogation unit amplifier and local oscillator noise [19]:

$$Loss(dB) = 40\log_{10} f + 40\log_{10} d + IL$$
$$-20\log_{10} G - 40\log_{10}\left(\frac{c}{4\pi}\right)$$

The graph showing the variation of loss(dB) with the distance d from the resonator is shown in Fig. 6.

Assuming a receiver detection limit of -60dBm (which takes into account the amplifier and local oscillator noise), we can have a maximum system loss of 70 dB. From Fig.6 this gives an allowable interrogation range of ≈3m (assuming isotropic antennas). However, using a directional interrogation unit antenna of 10 dBi, we can increase the interrogation range to about 10 m.

B. Propagation in dielectric, non-conducting media

The case of insulating media of non-unity relative permittivity is interesting because it relates to sensors buried in soil or plastic. An intuitive understanding of the propagation distance decrease when operating in dielectric media comes from the $\lambda^2/(4\pi)$ term in the FSPL expression: this term expresses the intersection of the sphere over which the energy spreads as the electromagnetic wave propagates (4π steradians) and the typical antenna dimensions of λ^2. Because in dielectric media of relative permittivity ε_r the wavelength is reduced by a factor $\sqrt{\varepsilon_r}$, the intersection area is reduced by ε_r and during the two way trip (interrogation unit to sensor and back) the FSPL increases by a factor ε_r^2.

C. Propagation in dielectric, conducting media

The case of conducting media is even worse, since the propagating wave becomes evanescent in high conductivity media such as sea water. As is well known [20], [21], [22], [23], such media is unsuitable to long range radiofrequency communication since the attenuation follows an exponential law expressed as follows: the major issue with electromagnetic wave propagation in conducting (e.g sea water) media is the energy loss due to the conductivity of the medium σ. By solving Maxwell equations, one identifies an exponential loss term with distance Z following $\exp(-\alpha \times Z)$ with

$$\alpha = \frac{\omega}{c_0}\sqrt{\frac{\varepsilon_r}{2}\left(\sqrt{1+\frac{\sigma^2}{\varepsilon^2\omega^2}}-1\right)}$$

where $\varepsilon = \varepsilon_0\varepsilon_r$, and $\varepsilon_0 = 8.85418782 \times 10^{-12}$ m^{-3} kg^{-1} s^4 A^2. The conversion to a logarithmic value, representative of the exponential decay of the electromagnetic wave in a conducting medium, and using $Z = 1$ for a normalized distance, as provided in [24], yields losses per unit distance of $8.7 \times \alpha$ dB/m since $20\log_{10}(e) = 8.7$ [25].

Two asymptotic conditions can be deduced from this general relationship which, as is, is rather difficult to grasp: the condition $\sigma \to 0$ and for large σ:

- in the former case, representative of low conductivity media (e.g. tap or river water), the losses are independent on the frequency since the term $\sigma/(\varepsilon\omega)$ vanishes, and the impedance rupture and free space propagation losses dominate. In this case, the wave is propagative and is hardly damped by the medium,
- in the latter case, the evanescent wave property dominates the propagative term, and the term $(\sigma/(\varepsilon\omega))^2$ dominates the +1 and -1 terms. By introducing angular frequency under the square root as well as the velocity in free space, remembering that $1/c_0 = \sqrt{\varepsilon_0\mu_0}$, we find that the conductivity losses are proportional to the square root of the conductivity and the frequency f: $\alpha \simeq \sqrt{\pi f \mu_r \sigma}$ (in non-magnetic media such as water, $\mu_r = 1$.

Notice from this last formula that the higher the frequency (assuming a conductivity driven loss and not effects associated with resonant modes of the water molecule as discussed in [24] – excluding any frequency above the GHz range in the process), the higher the conductivity-related loss. Numerical application shows that the losses are in the range of 0.1 dB/m for tap water to 100 dB/m for sea-water (conductivity of 5 S/m [26]), as validated by [24].

Another way of considering the typical interrogation range in a conductive medium is to compute the skin depth δ given by

$$\delta = \sqrt{\frac{2}{\mu_0\sigma\omega}}$$

where $\mu_0 = 4\pi \times 10^{-7}$ V.s/(A.m). The conductivity of sea-water is about $\sigma \simeq 5\,(\Omega.\mathrm{m})^{-1}$ so that the attenuation rate at 434 MHz yields a skin depth of 11 cm.

Furthermore, since the electromagnetic velocity v is dependent on both the relative permittivity ε_r *and the conductivity* σ, the wavelength also becomes dependent with these two parameters:

$$v = \frac{c}{\sqrt{\frac{\varepsilon_r}{2}\left(\sqrt{1+\frac{\sigma^2}{\varepsilon^2\omega^2}}+1\right)}}$$

where c is the velocity of an electromagnetic wave in free space. Although this term affects the velocity (and hence the wavelength) less than the relative permittivity, this additional parameter is significant in sea water, since it scales the wave by another factor of about 1.3 solely due to the conductivity of sea water, and hence can decrease the antenna efficiency if it was tuned for low-conductivity water.

Fig. 6 summarizes the various interrogation ranges expected from an interrogation unit operating in air, tap water or salt water. In addition, the case of the 10 dBi gain antenna was again reported: in all cases, the threshold detection limit is considered to be 70 dB (as shown by a horizontal black line). One way of compensating for the excessive losses in high permittivity media is to lower the operating frequency to return to the conditions we are familiar with in air. As an example of a reasonable target frequency when working with SAW devices, the case of 100 MHz sensors (33 cm-wavelength in water, half the 69 cm wavelength of the 434 MHz band in air) is summarized in Fig. 7.

Interestingly, [27] states a factor of two attenuation – or 6 dB – for each 3-cm distance of a 100 MHz RF electromagnetic wave propagating in a human body. Such a statement is consistent with our simulation (Fig. 7) since biological tissues exhibit conductivities in the 0.5 to 1.5 S/m range [28], hence

the reference stating an expected loss of 200 dB for a 1-meter propagation range agrees with the proposed graphs.

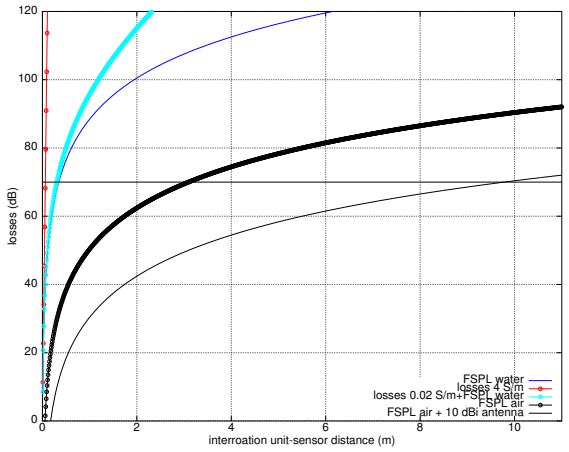

Fig. 6. Propagation (FSPL) and conductivity losses for a 434 MHz wave propagating in air or in water. Sea water was expected to exhibit a conductivity of 4 S/m, while tap water was assumed to be 0.02 S/m (in both cases, $\varepsilon_r = 80$).

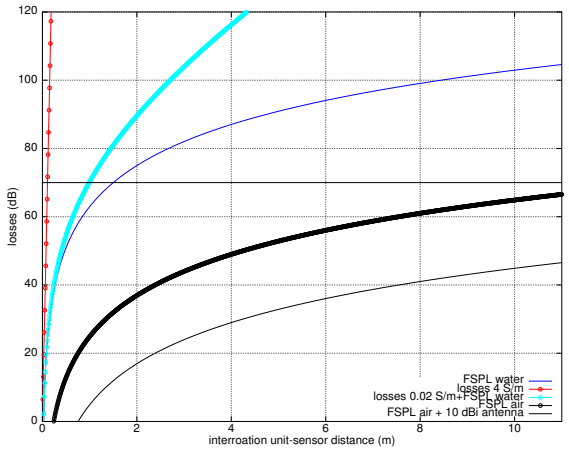

Fig. 7. Propagation (FSPL) and conductivity losses for a 100 MHz wave propagating in air or in water. Sea water was expected to exhibit a conductivity of 4 S/m, while tap water was assumed to be 0.02 S/m (in both cases, $\varepsilon_r = 80$).

V. Experimental Long Range Measurement Assesments

Two temperature sensors (SENSeOR, Besançon, France, reference SEAS10) were installed a double glazing window. The aim of the measurement is to assess the insulating capability of the double glazing window installation: while the indoor temperature is trivially measured as would be done with any wired sensor, the wireless passive sensor becomes a significant advantage when probing the outdoor temperature without drilling holes in the window pane. To demonstrate the long range measurement capability, the reader is located 10 m away from the sensors, fitted with a 7-element, 9 dBi gain, Yagi-Uda antenna (Fig. 8, top). The measurement has been continuously running since October 2011, with all missing data due to failures of the sink: a laptop computer recovering the data from the reader through a Bluetooth link will fail during power failure or internet connection loss. The outdoor data are compared with the records provided on the Weather Underground web site [29] by a weather station located less than 25 km away from the experiment site. Although the sensors were individually calibrated in a climatic chamber before installation, no additional data processing was performed on the records displayed in Fig. 8, bottom.

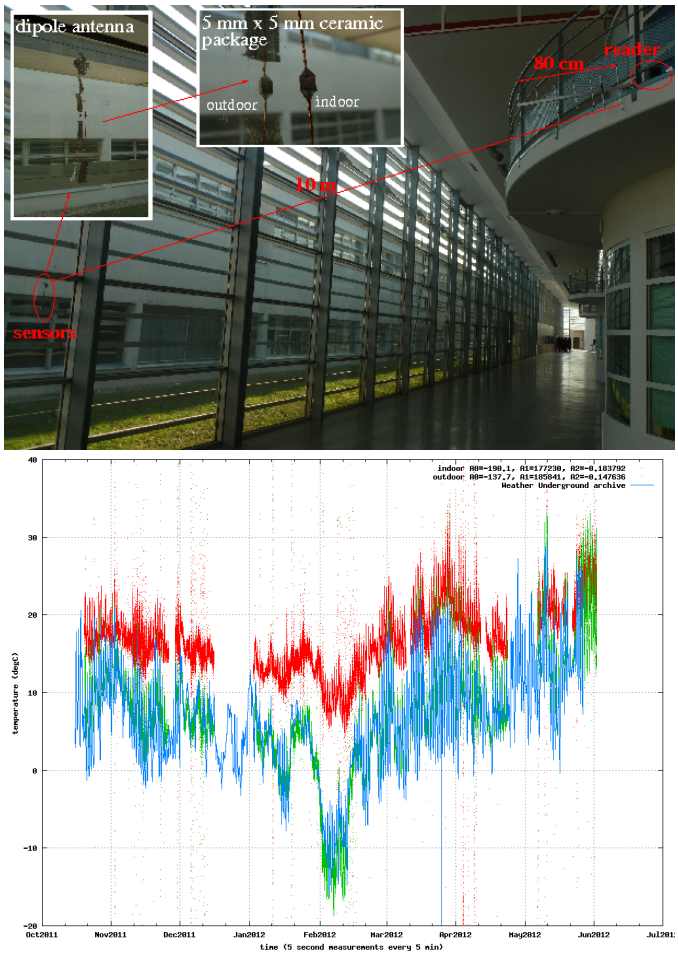

Fig. 8. Top: experimental setup. Two sensors are locatd outdoor and indoor on both sides of a double glazing window. The reader, located 10 m away from the sensors, probes the sensors through a Yagi-Uda antenna. The recorded data (indoor red, outdoor green) are compared with reference data from a weather station located less than 25 km away (blue).

VI. Conclusions

The theoretical and experimental modelling of a high Q SAW resonator transient response, working in the 433 MHz ISM band is done. Theoretical expressions are derived for the resonant/anti-resonant frequencies and the time constant, which are verified by ADS simulations. It is shown that the

resonator needs about 10 μs to charge/discharge appreciably. This is critical for designing proper RADAR waveforms for SAW resonator interrogation. Data gathered by theoretical calculations and simulations is used to calculate the possible range of resonator interrogation under different conditions, which are verified by actual measurements with an interrogation unit. Experimental demonstration is given of two sensors located inside and outside a double glazing window, probed from a distance of 10 m using a reader equiped with a directional Yagi-Uda antenna. The record has been running for more than 6 months and compared with reference data from a nearby weather station. It is hoped that the present work will provide wireless SAW sensor system designers with the necessary theory, simulation techniques and methodology to improve the performance of their designs.

REFERENCES

[1] C.-J. Lin, C.-W. Hung, and H.-P. Lin, "A study of wireless torque sensing based on saw sensors," in *Computer Communication Control and Automation (3CA), 2010 International Symposium on*, vol. 2, may 2010, pp. 211 –214.

[2] A. Karilainen, T. Finnberg, T. Uelzen, K. Dembowski, and J. Muller, "Mobile patient monitoring based on impedance-loaded saw-sensors," *Ultrasonics, Ferroelectrics and Frequency Control, IEEE Transactions on*, vol. 51, no. 11, pp. 1464 –1469, nov. 2004.

[3] G. Bruckner, A. Stelzer, L. Maurer, J. Biniasch, L. Reindl, R. Teichmann, and R. Hauser, "A high-temperature stable SAW identification tag for a pressure sensor and a low-cost interrogation unit," in *11th International Sensor Congress (SENSOR)*, Nuremberg, Germany, 2003, pp. 467–472.

[4] R. Fachberger, G. Bruckner, R. Hauser, and L. Reindl, "Wireless SAW based high-temperature measurement systems," 2006.

[5] D. Morgan, *Surface Acoustic Wave Filters*, 2nd ed. Elsevier, 2007.

[6] L. Reindl, G. Scholl, T. Ostertag, C. Ruppel, W.-E. Bulst, and F. Seifert, "SAW devices as wireless passive sensors," in *IEEE Ultrasonics Symposium*, 1996, pp. 363–367.

[7] W. Bulst, G. Fischerauer, and L. Reindl, "State of the art in wireless sensing with surface acoustic waves," *IEEE Transactions on Industrial Electronics*, vol. 48, no. 2, pp. 265–271, April 2001.

[8] H. Scherr, G. Scholl, F. Seifert, and R. Weigel, "Quartz pressure sensor based on SAW reflective delay line," in *IEEE Ultrasonics Symposium*, San Antonio, TX, USA, 1996, pp. 347–350.

[9] A. Pohl, R. Steindl, and L. Reindl, "The "intelligent tire" utilizing passive SAW sensors – mesurement of tire friction," *IEEE Transactions on Instrumentation and Measurement*, vol. 48, no. 6, pp. 1041–1046, december 1999.

[10] J. Beckley, V. Kalinin, M. Lee, and K. Voliansky, "Non-contact torque senseor based on SAW resonators," in *IEEE Int. Freq. Control Symposium and PDA Exhibition*, New Orleans, LA, USA, 2002, pp. 202–213.

[11] V. Kalinin, R. Lohr, A. Leigh, J. Beckley, and G. Brown, "High-speed high dynamic range resonant SAW torque sensor for kinetic energy recovering system," in *European Frequency and Time Forum (EFTF)*, 2010.

[12] Y. Dong, W. Cheng, S. Wang, Y. Li, and G. Feng, "A multi-resolution passive SAW chemical sensor," *Sensors and Actuators B*, vol. 76, pp. 130–133, 2001.

[13] D. Dye, "The piezo-electric quartz resonator and its equivalent electrical circuit," *Proc. Phys. Soc. London*, vol. 38, pp. 399–458, 1925.

[14] K. V. Dyke, "The electrical network equivalent of a piezoelectric resonator," *Phys. Rev.*, vol. 25, p. 895, 1925.

[15] J. Vig and A. Ballato, *Ultrasonic Instruments and Devices, Chapter 7*. Academic Press, Inc., 1999.

[16] J.-M. Friedt, C. Droit, G. Martin, and S. Ballandras, "A wireless interrogation system exploiting narrowband acoustic resonator for remote physical quantity measurement," *Rev. Sci. Instrum.*, vol. 81, p. 014701, 2010.

[17] G. Martin, P. Berthelot, J. Masson, W. Daniau, V. Blondeau-Patissier, B. Guichardaz, S. Ballandras, and A. Lamber, "Measuring the inner body temperature using a wireless temperature saw-sensor-based system," in *IEEE Ultrasonics Symposium*, vol. 4, september 2005, pp. 2089–2092.

[18] R. Brendel, , N. Ratier, L. Couteleau, G. Marianneau, and P. Guillemot, "Analysis of noise in quartz crystal oscillators by using slowly varying functions method," *Ultrasonics, Ferroelectrics and Frequency Control, IEEE Transactions on*, vol. 46, no. 2, pp. 356 –365, march 1999.

[19] N. Chrétien, J.-M. Friedt, S. Ballandras, B. F. cois, G. Martin, and P. Varshney, "On the need for low phase noise oscillators for wireless passive sensor probing," in *Sensorcomm 2012*, Rome, Italy, 2012.

[20] F. Yunus, S. Ariffin, and Y. Zahedi, "A survey of existing medium access control (MAC) for underwater wireless sensor network (UWSN)," in *Fourth Asia International Conference on Mathematical/Analytical Modelling and Computer Simulation*, 2010. [Online]. Available: http://trg.fke.utm.my/members/farizah/Paper1.pdf

[21] R. Collins, *Antennas and radiowave propagation*. Mcgraw-Hill College, 1985.

[22] D. Daniels, *Ground Penetrating RADAR, 2nd Ed.* Institution of Engineering and Technology, 2004.

[23] L. Liu, S. Zhou, and J.-H. Cui, "Prospects and problems of wireless communication for underwater sensor networks," *J. Wireless Communications and Mobile Computing – Underwater Sensor Networks: Architectures and Protocols*, vol. 8, no. 8, October 2008.

[24] J. Davis and A. Annan, "Ground penetrating radar for high resolution mapping of soil and rock stratigraphy." *Geophysical prospecting*, vol. 37, pp. 531–551, 1989. [Online]. Available: http://www.geosense.com/GPRmore.htm

[25] J.-M. Friedt, T. Rétornaz, S. Alzuaga, T. Baron, G. Martin, T. Laroche, S. Ballandras, M. Griselin, and J.-P. Simonnet, "Surface acoustic wave devices as passive buried sensors," *Journal of Applied Physics*, vol. 109, no. 3, p. 034905, 2011.

[26] R. Somaraju and J. Trumpf, "Frequency, temperature and salinity variation of the permittivity of seawater," *IEEE Transactions on Antennas and Propagation*, vol. 54, no. 11, pp. 3441–3448, 2006.

[27] A. Fenn, V. Sathiaseelan, G. King, and P. Stauffer, "Improved localization of energy deposition in adaptive phased-array hyperthermia treatment of cancer," *The Lincoln Laboratory Journal*, vol. 9, no. 2, pp. 187–196, 1996.

[28] R. Pethig, "Dielectric properties of body tissues," *Clin. Phys. Physiol. Meas.*, vol. 8A, pp. 5–12, 1987.

[29] http://www.wunderground.com/weatherstation/WXDailyHistory.asp?ID=IFRANCHE6.